# MRI-only Based External Beam Radiation Therapy of Prostate Cancer: Early Evaluation of Workflow and Clinical Impact

**Jean-François Cabana, M.Sc.[1]; Dany Thériault, Ph.D.[1,2,3]**

[1]Centre régional intégré de cancérologie de Chaudière-Appalaches (CRIC), Lévis, QC, Canada
[2]Centre de recherche du CISSS de Chaudière-Appalaches, Lévis, QC, Canada
[3]Département de physique, de génie physique et d'optique, Université Laval, Québec, QC, Canada

## Introduction

Treatment planning in external beam radiation therapy (EBRT) traditionally requires computed tomography (CT) images, with or without additional magnetic resonance (MR) images. These complementary imaging modalities both have properties that are useful or necessary for EBRT treatment planning.

On the one hand, CT provides excellent contrast for bone structures, but soft tissue contrast is limited. Furthermore, it is a requirement of treatment planning systems (TPS) to have a CT for accurate dose calculation. Modern TPS use a curve mapping CT number (or Hounsfield Unit (HU)-to-electron or mass density conversion), which is applied to patient CT data to allow for accurate calculation of energy transport and deposition in this heterogeneous environment. Moreover, a CT reference is also required for image guided radiation therapy (IGRT), either to generate digitally reconstructed radiographs (DRR) for kV imaging or as a direct reference for cone beam CT (CBCT) imaging.

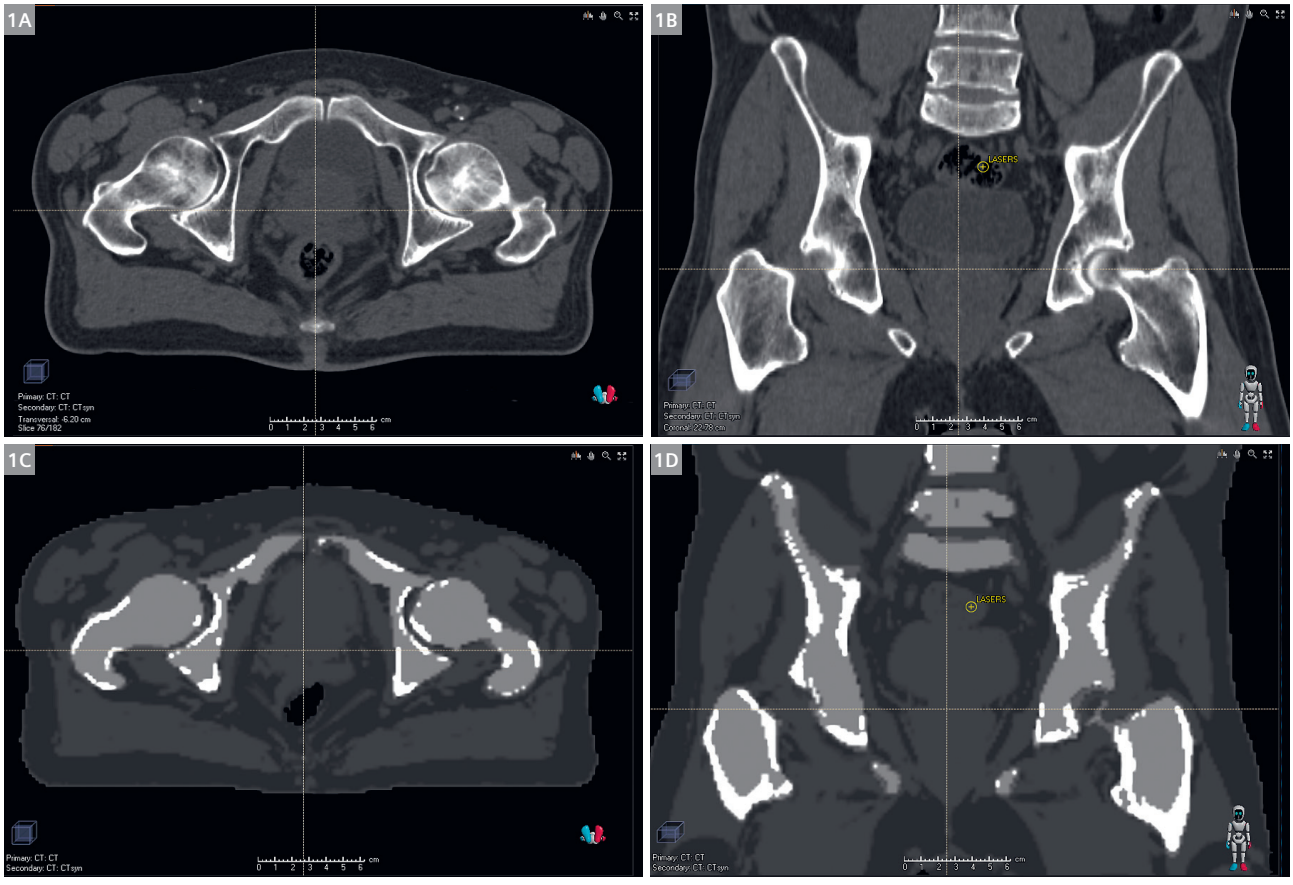


**1** Example of a sCT reconstruction. **(1A and 1B)** axial and coronal views of a planning CT; **(1C and 1D)** sCT images for the same patient.

On the other hand, MR imaging (MRI) offers a much better soft tissue contrast, and has the potential to add complementary information such as functional imaging. These advantages can help for more precise visualization and contouring of targets and organs at risk (OAR). MRI also does not use ionizing radiation, so no additional dose is given to the patient when using this imaging modality.

Working with the two imaging modalities in a complementary manner allows taking advantage of the strengths of both CT and MR, however, it does pose additional challenges. Registration of MRI to CT must be as accurate as possible to allow contouring on both image sets. Patient positioning must thus be reproducible in both CT and MR rooms. To do so, it is preferable to have a dedicated RT planning MR setup, including an RT table top overlay (i.e., a flat and indexable table top), MR compatible immobilization devices, an external laser bridge, and coil bridges to avoid direct contact with the patient which can deform patient anatomy. Despite compatible setups and proper patient positioning, registration can still be difficult, as there may exist residual differences in patient positioning between CT and MR sessions. In addition to this, CT and MR present completely different contrasts. Indeed, a structure perfectly visible on one image might not be easily seen on the other, making the visual registration difficult. Finally, there are often differences in the position and shape of internal organs as, for example, rectum and bladder filling can change between CT and MR image acquisitions. This all contributes to making it difficult in having an MR image that perfectly matches the CT image, and affect the overall geometric precision of the radiation therapy treatment to be administered. Using two imaging modalities also implies a heavier workload for the patient and department staff, as two examination sessions are needed.

## Synthetic CT

Recently, there has been increased interest in opting for MRI-only based treatment planning, particularly for prostate RT (see Bird et al. [1] for a publications review of clinical implementation of pelvic MRI-only planning). Planning on MR alone would mean that no registration is needed, while also allowing for a lighter workload for the patient. Because CT is required by TPS for dose calculation and during treatment for IGRT, one needs to replace the traditional CT image with something else to be able to perform RT planning without it. A potential solution is to generate a synthetic CT (sCT) image from the MRI. The idea is to use MRI to generate an image that has a contrast similar to CT, where pixel values are given in HU. Several strategies can be used to generate the sCT, and some commercial products are starting to become available.

Our clinic uses the synthetic CT product from Siemens Healthineers, which is available in their *syngo*.via software. The product is described in more details in the White paper [2]. In summary, this software uses specific MR sequences for sCT computation, which are available for the head and pelvic regions. For pelvic cases, a fast large field-of-view VIBE Dixon sequence is acquired (acquisition time around 2:30 minutes @ 1.5T), from which four images are output (in-phase, opposed-phase, water and fat). From these four images, soft tissue is segmented as water/fat/air using a classifier, while bones (2 densities) are rendered using a multi-atlas-based model. The result is a 5-compartment segmented sCT image, which is then imported in the TPS and recognized as a regular CT.

## Prostate EBRT at our center

The current workflow at our center for prostate EBRT planning is as follows. First, the patient is scanned at the MR (MAGNETOM Aera 1.5T, Siemens Healthcare, Erlangen, Germany) in treatment position. Our current prostate MR protocol consists of a single T2 3D sequence (T2-SPACE @ 0.8 mm isotropic resolution, acquisition time around 9 minutes). Then, treatment simulation is performed in the CT room (SOMATOM Confidence, Siemens Healthcare, Forchheim, Germany). CT and MR images are then imported into our TPS (RayStation 7, RaySearch Laboratories, Stockholm, Sweden), where registration between MR and CT is performed (with focus on the prostate). OAR are contoured by radiation therapists on the CT image, using the registered MRI as reference. These contours are verified by the radiation oncologist, who then contours the prostate and seminal vesicles on the CT, again using the MRI as reference. The treatment plan optimization, using a single full arc VMAT 6MV beam, is then performed on the planning CT image. Before each treatment session, a CBCT is acquired at the linac (Elekta Versa HD, Elekta AB, Stockholm, Sweden) and registration is made against the planning CT using Elekta XVI software.

## Project scope

Switching to an MRI-only workflow is a major change and we should expect it to come with some challenges along the way. The scope of the project presented here was thus to perform a preliminary evaluation of the workflow and clinical impacts of using an MRI-only process for prostate EBRT planning. The MR sequence for pelvic sCT reconstruction was added to our regular prostate protocol. This additional sequence was run only after obtaining patients' consent after the regular protocol was completed. We selected the first 12 patients for whom the sCT sequence was successfully acquired.

The goal was not to perform a full commissioning of the MRI-only workflow, but to identify:
(1) pitfalls and challenges at each step of the treatment chain;
(2) questions which still need answers, and
(3) the next steps required before making the transition.
To keep things simpler to start with, we focused on the treatment of prostate with seminal vesicles (SV) only (no treatment of pelvic nodes included).

The project was a collaborative effort between medical physicists, radiation oncologists, and radiation therapists. It is important to note that the observations made here are relevant to the workflow we use at our own center. It is advisable that each center performs their own evaluation to identify challenges specific to their clinic. The following sections present a brief summary of the methods used and results obtained for each of these steps.

## Imaging

### Method

Images from the 12 patients included in this study were qualitatively analyzed to evaluate image quality and sCT reconstruction accuracy. First, the general appearance of the reconstructed sCT was evaluated, then each sCT was compared to the actual planning CT. Bone registration between sCT and CT was performed first, followed by registration with respect to the prostate, as is done in our current CT+MR workflow.

### Results

First results showed that sCT reconstruction generally works quite well. See Figure 1 for a comparison between sCT and planning CT for one patient. A good agreement overall is seen for all tissue compartments between sCT and CT. sCT shows a clear difference between muscle and fat, and air pockets inside the rectum or bowels are well reconstructed. The two-density bone structures are clearly visible on the sCT, and agree with what is seen on the CT. Compared to the planning CT, sCT has a lower resolution, and only 5 HU levels. These characteristics combine to give an appearance that looks unnatural when compared with the planning CT.

Registration between sCT and planning CT confirmed that obtaining a reproducible patient positioning between MR and CT modalities could be difficult. Differences in external contours of up to 1 cm were not uncommon; rotation of pelvis/hips was sometimes seen, as well as differences in leg positions; changes in bladder and rectum filling were also seen for most patients. Registration with respect to the prostate required translations of up to 1 cm compared to bone registration. These observations confirm

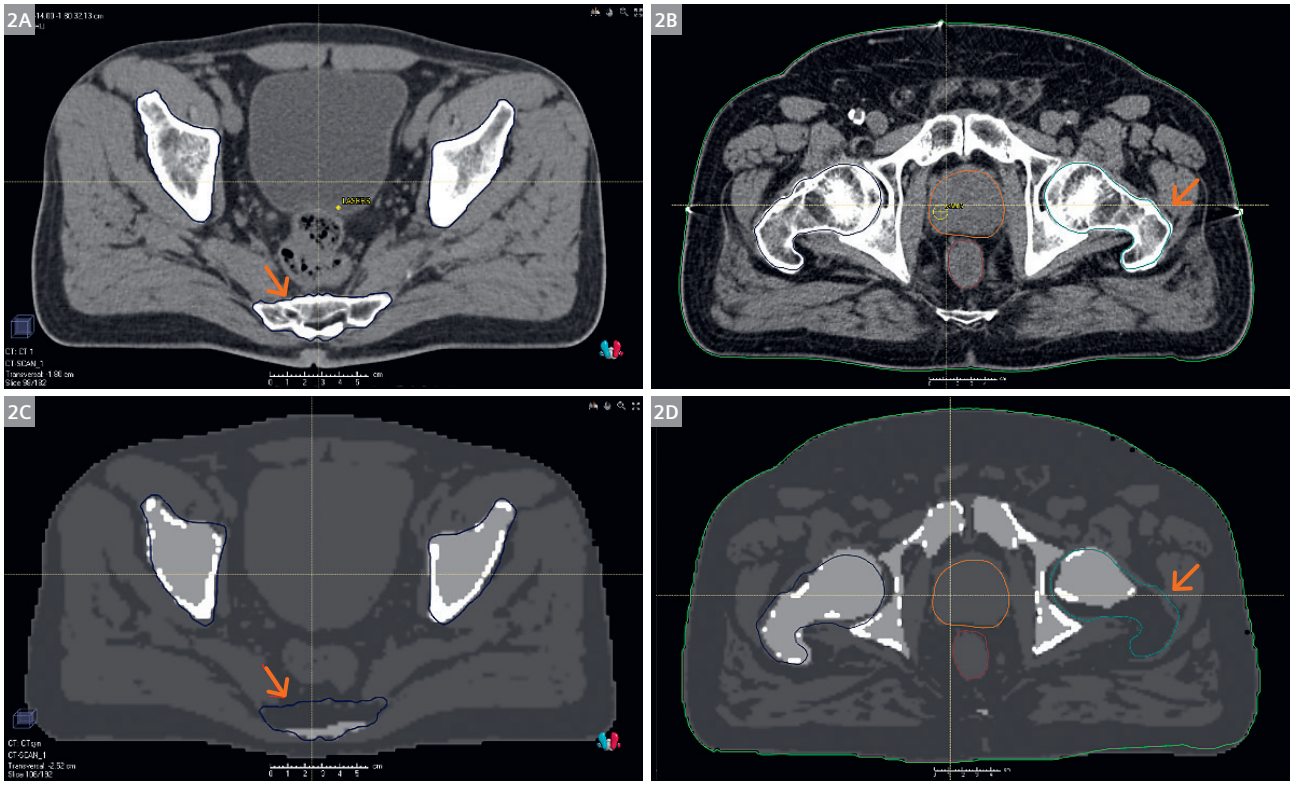


**2** Misreconstruction of some bone structures. **(2A and 2B)** planning CT images; **(2C and 2D)** sCT images for the same patient. Arrows point to bone structures that are incorrectly rendered on the sCT.

an advantage of using an MRI-only workflow, as the sCT is intrinsically registered to the MR images.

Careful inspection of sCT images also showed some limitations of the reconstruction. Nine out of 12 patients had some sort of misreconstructions in bone structures (see Figure 2). Most of these misreconstructions were limited to a small missing portion at the tip of the sacrum. However, one of these patients had a larger part of the sacrum missing. For another patient, some parts of the femoral heads were also missing. Another limitation is that calcifications are not reconstructed. Those calcifications are oftentimes useful for the registration during treatment, as they usually provide good contrast on the CBCT.

Some patients external contour was not fully included in the FoV, which showed the importance of proper placement of scan limits, and screening of patients that might be too large to be included fully in the MR FoV (50 cm FoV on the MR, vs. 70 cm for the CT).

Other artifacts which sometimes occurred included breathing artifacts on the abdomen (six out of 12 patients) getting incorrectly reconstructed as tissue, and air pockets at unusual places (e.g, in the bladder) for two patients (see Figure 3).

**Discussion**

Our first contact with sCT reconstruction showed a good overall agreement with planning CT. Fat and muscle compartments were well represented, despite some misreconstructions in the bones. A more thorough investigation would be needed to identify what could have caused the problems which we have encountered. As the bones are rendered using a multi-atlas-based model, it is possible that their proper reconstruction is sensitive to differences in patient positioning or scan limit placement.

Other artifacts were also seen, such as breathing artifacts on the abdomen, and tissue incorrectly assigned to air density. It is important to mention however, that most of these artifacts were easily identified when looking at source MR images. In these cases, they could be corrected inside the TPS by contouring on the MR images and assigning the correct density to those structures. Moreover, in most cases artifacts appeared outside of the region intercepting the beam, and would have no clinical impact on the treatment plan.

These early results showed the need to establish image quality checklists before we can start using these images alone for treatment planning. MR and sCT images should be reconstructed and inspected immediately following the MR session to assess image quality before the patient can leave the clinic. Acceptance criterion

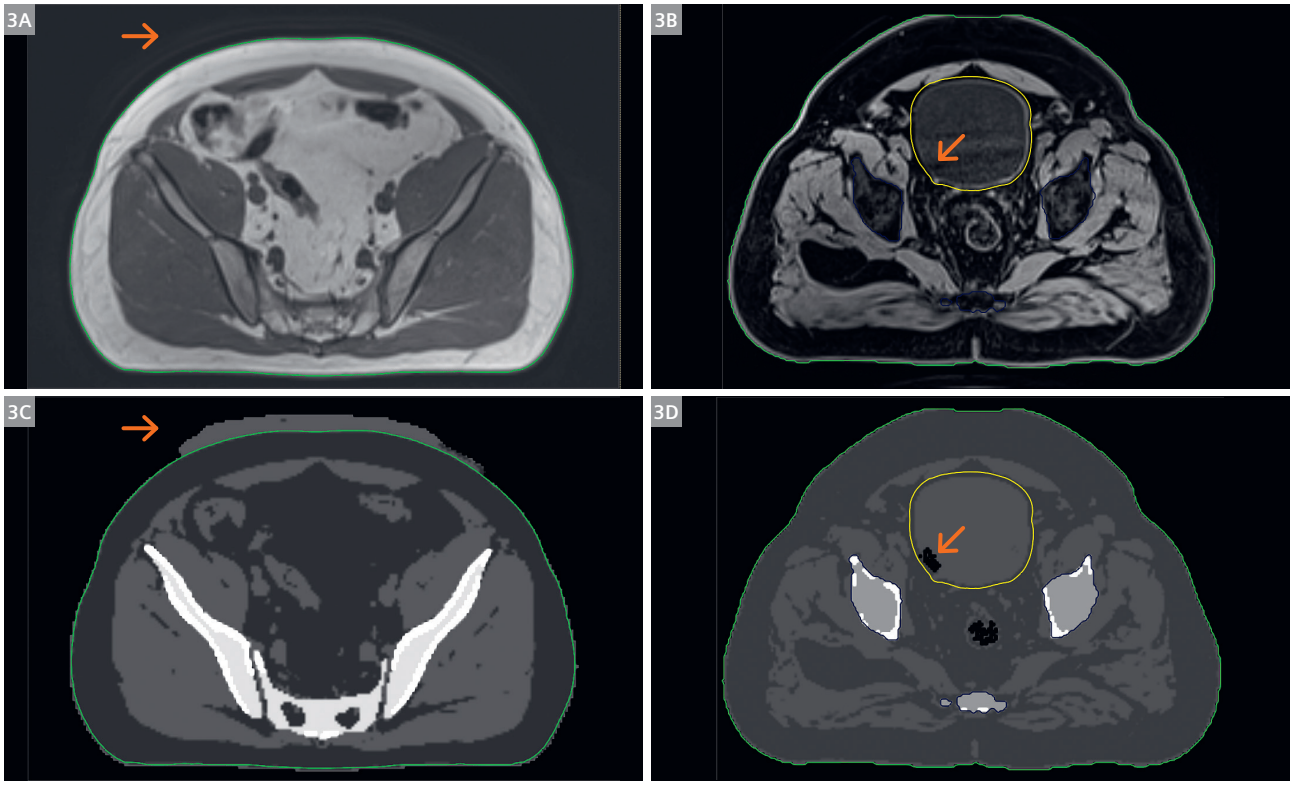


**3** Other sCT artifacts. **(3A and 3C)** the arrow shows where ghosting, caused by respiratory movement on the abdomen, was incorrectly rendered as muscle on the sCT. **(3B and 3D)** ghosting inside the bladder is incorrectly rendered as air.

should be established, and therapists should be ready to have the patient undergo a regular planning CT in case images are of poor quality or the sCT reconstruction fails.

## Imaging – geometric distortions in MR

CT images can be considered to be spatially accurate, but MR images are affected by geometrical distortions due to main magnetic field inhomogeneities, patient-induced susceptibility effects, gradient non-linearity, and eddy currents. These distortions must be small enough to ensure accurate OAR and target contouring. The goal of this part of the study was to quantify the distortions on MR images used in prostate planning and evaluate the impacts on the MRI-only workflow.

### Method

We used a custom MRI distortion evaluation phantom, based on the work from Walker et al. [3]. The phantom consists of a stack of PVC foam panels holding arrays of markers (fish oil capsules) visible on CT and MR images arranged over a polar grid, centered on the MR axis. A CT scan and an MR scan were both performed on the phantom. Images were imported in RayStation, where a rigid registration was first performed on the central region of the phantom (a 5-cm radius sphere around magnet isocenter), where distortion is assumed to be lowest. A deformable registration from MR images to CT was then performed over the whole phantom. This deformation is represented by a deformation vector field. The magnitude of the deformation vector at each point gave an indication of the geometric distortion induced in the MR image.

Distortion assessment was done for the T2 SPACE and the VIBE Dixon in-phase image. All patients' sCT images were registered to the phantom using the MR scanner isocenter position. Patient regions of interest (targets and OAR) were copied over on the phantom CT image. Displacement vector field statistics were obtained in those volumes to assess maximum distortion inside a subset of relevant anatomical structures: prostate (CTV), rectum, femoral heads, and complete external contour. From previous analyses, we know that distortion becomes greater at the edges of a very large FoV image. In this study, distortion was only relevant in the region intercepting the treatment beams. Thus, for the external contour, distortion was analyzed only over a section of 15 cm in the superior-inferior direction. This section covered all patient targets + 4 cm on each side in this direction, so the whole VMAT beam is entirely comprised in this region. For each ROI, distortion was analyzed on the image on which it had been contoured: T2 SPACE for CTV and rectum, and VIBE Dixon in-phase image for femoral heads and external. The maximum and the 95$^{th}$ percentile displacement values were analyzed.

### Results

Table 1 shows the patient-averaged maximum and 95$^{th}$ percentile distortion, as well as overall maximum displacement over all patients, for some regions of interest.

Inside the CTV and OAR, the global maximum distortion over all patients was less than 0.2 cm, while the 95$^{th}$ percentile was 0.1 cm or less. Inside the patients' external contour, the global maximum was close to 0.5 cm, with a 95$^{th}$ percentile of less than 0.15 cm.

### Discussion

Based on the results above, it appears that geometric distortion for our MRI sequences can be kept reasonably low inside the target and OAR (maximum of 0.18 cm, and a 95$^{th}$ percentile of 0.1 cm or less). This level of uncertainty seems acceptable for prostate treatment planning. Moving further away from the magnet isocenter, distortion becomes greater, and can reach close to 0.5 cm overall within the patient's body outline. This again seems reasonable as the effect of

[1] *Distortion values depend on field strength and acquisition protocol (e.g. in-plane acquisition pixel size or acquisition readout pixel bandwidth), therefore, measured values may differ at various sites.*

| Deformation statistics – Average and global maximum for all 12 patients[1] | | | | |
|---|---|---|---|---|
| **ROI** | **Image** | **Maximum distortion (patient average) [cm]** | **95$^{th}$ percentile distortion (patient average) [cm]** | **Maximum distortion (overall) [cm]** |
| CTV | T2-SPACE | 0.14 | 0.09 | 0.16 |
| Rectum | T2-SPACE | 0.13 | 0.08 | 0.16 |
| Left femoral head | Dixon in-phase | 0.18 | 0.10 | 0.18 |
| Right femoral head | Dixon in-phase | 0.16 | 0.10 | 0.18 |
| External body contour | Dixon in-phase | 0.39 | 0.14 | 0.47 |

**Table 1:** Overall distortion[1] statistics inside patients' target and OAR volumes.

the difference in external contour will be spread out over a complete VMAT arc, and should have no significant impact on the dose delivered to the target volume or OAR.
There are some limitations worth mentioning in this analysis. First, the method employed is limited by the accuracy of the deformable registration algorithm. It was observed in this study that the choice of deformation grid size had an impact on registration. The grid size was chosen empirically to obtain the best possible visual match between the two images after registration. Another limitation of the method is that there is no image information in empty spaces between the markers in our phantom. The choice of distance between markers could have an impact on the deformation vector field, although this field is expected to be spatially slowly varying.

To evaluate the reproducibility of the method, the phantom was scanned at the CT using the same imaging parameters on two separate sessions. Ideally, performing the rigid and deformable registration analysis should result in no displacement between the two image sets. Results showed a maximum displacement of 0.07 cm within the CTV, and 0.085 cm inside the patients' external contour. This displacement is indeed very low, but not zero, which demonstrates some uncertainty of the results.

Finally, one important limitation of distortion evaluation using a phantom is that it does not take into account specific patient-induced susceptibility distortions. The phantom used in this study is very large to cover a larger FoV, and was not made to be representative of a patient anatomy. It is likely that results would be slightly different for each individual patient.

## Target volume contours

In our current workflow, MRI is registered to CT, with emphasis on the prostate. A radiation oncologist then contours the prostate and seminal vesicles (SV) on the CT image, with the MR T2-SPACE image to assist, as the MR gives a better visibility for the base, apex, and anterior wall of the prostate. In an MR-only workflow, no CT would be available for contouring. The question is then to determine whether using only MRI for contours will change how the prostate is delineated.

**Method**
A radiation oncologist was asked to contour the prostate and SV for the 12 patients using T2-SPACE images only. These patients had already been treated, so a prostate contour made using CT was already available. Total volume of these structures were compared between CT+MR and MR-only contours. Automatic segmentation was also performed on the prostate to divide it in 6 subregions (superior, inferior, left, right, anterior, and posterior). Differences in contours between CT+MR and MR-only in these subregions were compared separately to determine if there were differences in some preferable directions.

**Results**
Table 2 shows results for the overall target volumes. These results show that both the prostate and SV have smaller volume when contoured on MRI alone vs. CT+MRI. On average, the prostate was 2.7 cc smaller (-7%; p-value = 0.038), and the SV 1.7 cc smaller (-14%; p-value = 0.007). The maximum absolute difference for a single patient was -11.6 cc for prostate and -4.5 cc for SV.

Differences in volumes were also analyzed separately for 6 regions (left, right, ant, post, sup, inf). Table 3 shows the results of this analysis. Intersubject variability was high, but statistically significant differences were observed in anterior and superior regions, where the volume was found to be smaller for MRI. The mean volume difference was of -1.33 cc (p = 0.048) and -1.59 cc (p = 0.015) for the anterior and superior regions, respectively.

**Discussion**
Contouring targets on MRI alone vs. CT+MRI has an impact on the volume contoured. Overall volume was smaller for prostate and SV when contoured on MRI alone. On average,

| | Prostate | | | | Seminal vesicles | | | |
|---|---|---|---|---|---|---|---|---|
| ID | CT+MR volume [cc] | MRI volume [cc] | Difference [cc] | Relative difference [%] | CT+MR volume [cc] | MRI Volume [cc] | Difference [cc] | Relative difference [%] |
| Min | 22.6 | 21.4 | -11.6 | -23% | 6.6 | 4.3 | -4.5 | -34% |
| Max | 72.6 | 75.9 | 3.3 | 8% | 18.0 | 19.9 | 2.0 | 11% |
| Mean | 43.0 | 40.3 | -2.7 | -7% | 12.8 | 11.2 | -1.7 | -14% |
| p-value | 0.038 | | | | 0.007 | | | |

**Table 2:** Overall volume comparison of the prostate and seminal vesicles.

| ID | Left [cc] | Right [cc] | Ant [cc] | Post [cc] | Sup [cc] | Inf [cc] |
|---|---|---|---|---|---|---|
| Min | -2.69 | -1.50 | -3.90 | -3.05 | -3.74 | -4.60 |
| Max | 1.09 | 1.49 | 1.87 | 3.04 | 3.26 | 2.46 |
| Mean | -0.18 | -0.08 | -1.33 | 0.56 | -1.59 | -0.74 |
| p-value | 0.547 | 0.723 | 0.048 | 0.291 | 0.015 | 0.192 |

**Table 3:** Directional volume difference (+: MRI larger).

the differences were found to be small, but they can be large on an individual basis. For the SV, the difference was considered to have no clinical impact, as only 1 cm proximal to the prostate is included in the treatment.

We found that prostate volume was slightly smaller in anterior and superior regions, but again the difference was small on average. Because prostate boundaries are better visualized on MRI, it is more likely that contours on CT are slightly larger than they need to be, instead of the other way around. Based on these results, we felt confident going forward with contouring on MRI alone.

## OAR contours

Not having an actual CT image to perform OAR contours implies that these contours would need to be done using only MR images and possibly the sCT image. The evaluation for this step of the workflow aimed to identify pitfalls and areas needing improvement in our imaging protocol.

### Method

Therapists contoured OAR on five selected patients using all MR images available (T2-SPACE and all four Dixon images from the sCT sequence) as well as the sCT itself (see Figure 4). They were instructed to use any images that they found to work best for each OAR and to take note of their observations. OAR contoured for prostate planning include rectum, bladder, small bowel, penile bulb, pelvis, femoral heads, external genital organs, and cauda equina.

### Results

Qualitative observations were made regarding image quality and OAR visibility. For the rectum, T2-SPACE, Dixon in-phase and sCT were found to be useful. It was noted that visibility was suboptimal in the most inferior section. The bladder was easily seen on all images, but was not fully encompassed on the T2 image due to limited FoV. It was also noted that there could be filling of the bladder between the Dixon and T2 sequences. The small bowel was easily seen as well, and could be drawn directly on the sCT image using the Dixon fat image to remove muscles. The penile bulb was found to be more easily seen on the T2 image. External genital organs were easily seen directly on the sCT, using any other image as a reference if needed. Pelvis and femoral heads were very easy to contour on the sCT using automatic segmentation tools, as the image is comprised of discrete HU levels. Misreconstructions on the sCT could be corrected using other images. The cauda equina was found to be very difficult to see on all MR images, and the quality of the sCT was insufficient in the sacrum region to allow proper contouring of this structure.

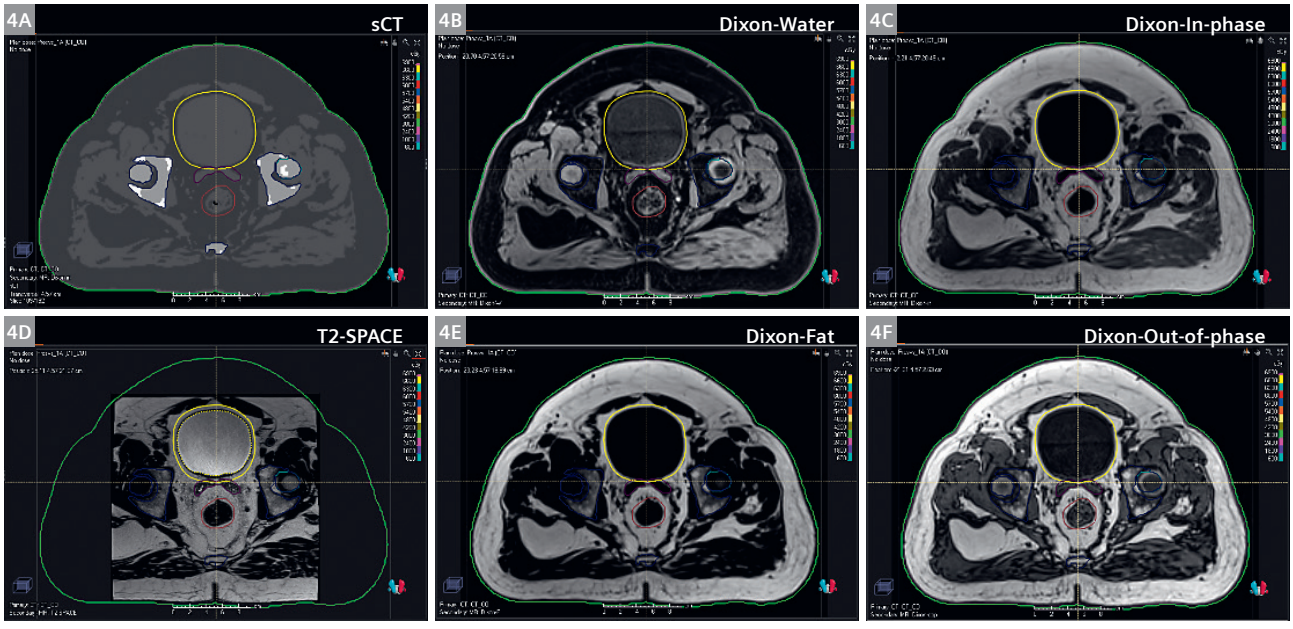


**4** An example of all images available from our MR protocol for a single patient.

**Discussion**
Most OAR could be easily contoured using available images. For the clinic workflow, we would need to standardize which image(s) to use for each OAR. This evaluation allowed identifying areas needing improvement. In particular, it was found that the T2-SPACE sequence could be improved for better visibility of the rectum. We could also try to increase resolution on the Dixon sequence to get better visibility of the cauda equina. However, for treatment of the prostate alone, cauda equina is rarely a critical OAR, so an approximate contour should be sufficient in this case.

## Plan optimization and dose accuracy

Following the imaging session as well as OAR and target volume contouring, the next step in the workflow is to optimize the treatment plan itself in the TPS. In this preliminary testing phase, we evaluated if the usage of the sCT would induce changes in the plans that are produced. There are two elements that were evaluated. First, would working on a sCT change how dosimetrists work, and are there pitfalls in the workflow? Second, is the dose calculation in the TPS different when working on the sCT vs. the regular planning CT?

**Method**
For the workflow and plan optimization evaluation, five therapists worked from scratch on five different cases, planning a regular prostate + SV treatment. The dose prescription was 60 Gy in 30 fractions, using a single-arc 6MV VMAT beam. The instructions given were to optimize the plans just as they normally would and note any relevant observations.

For the dose accuracy evaluation, original treatment plans (planned on regular CT) for all 12 patients were recalculated on the sCT. To mitigate the effect of differences in the patients' external contour (caused by differences in positioning during imaging sessions or geometric distortions on the MR images), areas where body outline was larger on the sCT were overridden with air density, while areas where the outline was smaller on the sCT were overridden with adipose density.

To allow for a direct comparison of dose distributions and eliminate differences in internal organ shapes, contours (targets and OAR) from the planning CT were copied directly on the sCT. Dose difference distributions were then evaluated visually, and dose volume histograms (DVH) were analyzed in some structures of interest (CTV, PTV, rectum, bladder, and femoral heads).

**Results**
***Plan preparation and optimization***
Some missing details were observed during the plan preparation and optimization stage. First, it was noted that the localization point, which represents the point of intersection of the lasers, could not be placed on the sCT. It is usually identified on the CT by placing radio-opaque markers on the patient's skin. In our traditional CT+MRI workflow, no markers are used during MRI. As such, the localization point was not identifiable on MR images.

Another difficulty was that the examination table is not visible on the MRI. Usually, a table structure modeled for accurate beam attenuation is predefined in the TPS. This structure is placed manually according to its position visible on the planning CT. As the table is not visible on MR images, it was impossible to position the structure accurately on the sCT.

Similarly, positioning accessories (namely an indexable board placed on the table) are not visible on the MRI. In the traditional workflow, all accessories are included within the patient's body outline, so that beam attenuation is properly taken into account. In this study, as the accessories were not visible, they could not be included.

Some qualitative remarks were also pointed out by dosimetrists, mostly regarding visual appearance of the sCT. Some felt that they were not dealing with a real patient because of the segmented appearance, while others thought that OAR contours looked less accurate because of the lower resolution. No issues were observed with regard to the plan optimization process, and they found that the plans optimized on the sCT were of equal quality to those optimized on a regular CT. Final dose distributions were qualitatively similar.

***Dose accuracy***
For the reasons mentioned above regarding equipment not visible on MRI, table and accessories were excluded from the regular CT to allow a direct comparison between plan dose calculated on the sCT vs. CT.

Having no specific HU to mass density curve for the sCT, the same curve as the regular planning CT was used in the first phase of this evaluation. Table 4 shows the difference in CTV average dose using this curve. Initial tests showed that CTV average dose on sCT was 1.3% higher (averaged over all patients), with a maximum difference

| | "Water" = 1.0 g/cm$^3$ | "Water" = 1.05 g/cm$^3$ |
|---|---|---|
| Min | 0.5% | -0.5% |
| Max | 2.1% | 0.9% |
| Mean | 1.3% | 0.1% |

**Table 4:** CTV average dose difference for different densities of the "water" compartment (sCT dose - CT dose).

of 2.1% for two out of twelve patients. A possible explanation is that the "water" compartment on sCT corresponded mostly to muscles, which has a slightly higher density than water (around 1.05 g/cm³ for muscle instead of 1.0 g/cm³ for water). This compartment was thus segmented on the sCT and assigned muscle density. Using this density, CTV average dose on sCT was 0.1% higher (averaged over all patients), with a maximum difference of 0.9% for one patient.

Having found that the dose difference was lower with muscle density assigned to the water compartment, this density was kept for the following comparison. Dose difference distributions showed that local differences were in general well below 1% of the prescription dose (see Figure 5 for a representative sample). No significant difference was found on the DVH curves of all evaluated contours (targets and OAR).

Table 5 shows average, min, and max differences for some relevant DVH points (sCT - CT) evaluated over all patients. The average maximum difference was found to be 0.31% for the D1% in the PTV. The maximum absolute difference (for a single patient) was of 1.15%, again for the D1% in the PTV.

## Discussion

This preliminary evaluation showed that, with proper densities applied to all five sCT segmented compartments, it is possible to obtain a dose distribution that is very similar to that planned with the regular CT. Maximum local differences were less than 1% of the prescription dose, and DVH curves were visually indistinguishable between CT and sCT. Maximum differences on the DVH indices were for the PTV D1%, which corresponds to the plans' hot spots inside the target volume. These observations suggest that no uncertainties of clinical relevance result from the dose computation on a sCT vs. a regular CT.

A few issues will need to be addressed in the simulation step, before we are able to plan solely on the sCT. First, we will need to test MRI markers (commercial markers or off-the-shelf oil capsules) to identify properly

| | Average | Min | Max |
|---|---|---|---|
| Femoral Heads D1% | 0.15% | -0.62% | 0.75% |
| Femoral Heads mean | 0.00% | -0.25% | 0.21% |
| PTV D1% | 0.31% | -0.92% | 1.15% |
| PTV D99% | 0.14% | -0.67% | 0.80% |
| PTV mean | 0.24% | -0.66% | 0.78% |
| Rectum D1% | 0.09% | -1.09% | 0.68% |
| Rectum mean | -0.04% | -0.23% | 0.13% |
| Bladder D1% | 0.17% | -0.57% | 0.76% |
| Bladder mean | -0.06% | -0.20% | 0.02% |

**Table 5:** Average, min, and max differences between sCT and CT of selected DVH points.

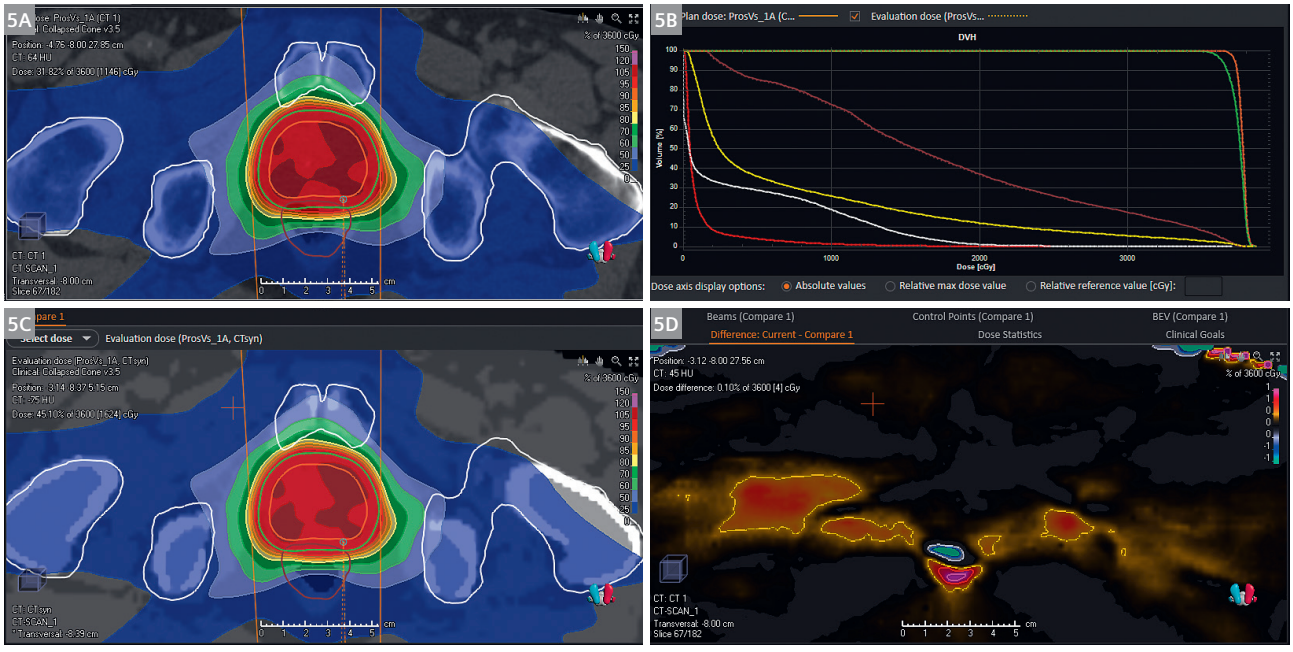


**5** Example of a dose distribution computed on planning CT **(5A)**, and the same plan computed on sCT **(5C)**. Dose difference (CT - sCT) is shown at bottom right **(5D)** (scale goes from -1% to +1%). DVH curves are presented at the top right **(5B)** (solid lines = CT, dashed lines = sCT). Green: PTV; Orange: CTV; Brown: Rectum; Yellow: Bladder; White: Pelvic bones; Red: Small bowels

the laser localization point on patients. Second, we should establish a procedure to properly identify table position (not visible on MR images), which could be as simple as measuring the height of the lasers with respect to the table top. Finally, we need to determine how to consider beam attenuation through positioning accessories. For example, a new table structure could be included in the TPS that takes into account the outline and attenuation of standard accessories.

## IGRT treatment

Workflow in our clinic for prostate treatment includes a daily CBCT, which is registered on the planning CT. As was noted above, the sCT has quite a different appearance than the CT. The question here was thus to evaluate how using a sCT as a reference would affect the registration.

**Methods**

Five patients for which sCT and CT images agreed well (with respect to patient positioning and internal organs) were selected, in order to have an accurate reference registration between those two images. Five therapists then performed three registrations each on all five patients: one from sCT to planning CT (sCT→CT), another from CBCT to planning CT (CBCT→CT), and finally from CBCT to sCT (CBCT→sCT). The sCT→CT registration was taken as a "true" reference, to which CBCT registrations were compared. Only translations were allowed and all registrations were done manually (no automatic registration).

For each patient, standard deviation on registration results across therapists is evaluated to assess variability. This variability was compared between CBCT→sCT and CBCT→CT registrations. From the CBCT→sCT and CBCT→CT registrations, an implicit sCT→CT registration was obtained. This implicit registration was then compared to the reference sCT→CT registration.

**Results**

Table 6 shows the inter-user standard deviations in each direction (average over 5 patients) of the CBCT→CT and CBCT→sCT registrations. In each direction (RL = Right-Left; IS = inferior-superior; PA = posterior anterior), the standard deviation was slightly higher for the CBCT→sCT registration. However, none of those differences was found to be statistically significant ($p>0.05$).

Table 7 shows average differences in translation between the implicit and the reference sCT→CT registrations. Differences were of 0.042 cm, -0.127 cm and -0.021 cm in the RL, IS, and PA directions respectively. Only the difference in IS was found to be statistically significant, although this difference was small (less than 0.15 cm).

**Discussion**

From these preliminary results, there does not seem to be major differences using planning CT or sCT for registering CBCT. The only statistically significant difference was found to be a small (<0.15 cm) shift in the IS direction. It can be noted that the registration was performed by using not only a visual match between the images, but also by including target contours as a reference. Therefore, it is possible that differences seen earlier in target volume contours could affect how registration is done.

This part of our preliminary work was limited by a small sample size (5 therapists, 5 patients). Moreover, for simplicity, the registrations were performed in the TPS (RayStation), while registration in a clinical scenario would be made in different software (Elekta XVI). Also, registration in this evaluation were all manual, whereas in the clinical workflow an automatic bone registration is first performed, before manual corrections are applied. To get a clearer picture of the impacts of using sCT for IGRT, next steps would require a larger sample size and using the full clinical treatment workflow.

**Conclusion**

This study aimed to evaluate the impact on the clinical workflow of prostate EBRT planning when transitioning from a CT+MR to an MR-only workflow. Several steps in the complex treatment chain were examined, namely imaging, target and OAR contouring, plan optimization and dose calculation, and finally CBCT registration for IGRT. This evaluation allowed us to identify areas needing improvements before safely making the transition. While the results presented here are specific to the workflow used in our own center, some observations could be relevant for other centers.

| | RL [cm] | IS [cm] | PA [cm] |
|---|---|---|---|
| CBCT→sCT | 0.096 | 0.200 | 0.170 |
| CBCT→CT | 0.069 | 0.175 | 0.127 |
| Difference | 0.027 | 0.026 | 0.043 |
| p-value | 0.079 | 0.498 | 0.195 |

**Table 6:** Average inter-user standard deviation for CBCT registrations.

| | RL [cm] | IS [cm] | PA [cm] |
|---|---|---|---|
| Average difference | 0.042 | -0.147 | -0.021 |
| p-value | 0.079 | 0.022 | 0.635 |

**Table 7:** Difference in implicit vs. reference sCT→CT translations.

In particular, we found that image quality should be assessed directly after imaging at the MR, in case a fallback planning CT would be necessary. We discussed the importance of MR image geometric distortion assessment; this is something that should be done in each center at the time of commissioning, and as part of a periodic QA program. Differences in target volumes were observed when contours were made using only MRI. These differences were attributed to better visibility of the anterior wall and base of the prostate as seen on the MRI. Some areas needing improvement were noted for the OAR contours. It was found that the use of a sCT instead of a regular planning CT would have no significant impact on plan optimization and dose calculation in the TPS, as long as an appropriate HU-density curve is determined. Finally, a small difference in inferior/superior direction was found in the registration of the CBCT when matched against the sCT instead of the planning CT. This difference could be attributable to differences in target contours, although a more thorough investigation would be needed.

Next steps in the study would be to make adjustments necessary in each part of the chain as were presented above. We would then need to establish clear guidelines and protocols about the usage of the sCT. In a second phase of the study, we could perform end-to-end testing of the MR-only workflow. Patients could then continue to undergo both MRI and CT as a backup. Treatment plans could be made entirely on sCT, and then recalculated on CT at first for a sanity check.

In conclusion, this study showed that MRI-only based radiation therapy of prostate cancer is possible, with some adjustments needed at each step of the planning process. The transition must be planned very carefully, and impacts should be well understood and documented. As with any major change, we anticipate that workload for physicists and therapists could be increased at first, as everyone gets accustomed to the new workflow. Overall, this study gave our center a clearer picture of what needs to be done to make a safe and optimal transition to an MR-only workflow.

## Contact

Jean-François Cabana
Physicien médical clinique
Centre Régional Intégré de Cancérologie
de Lévis – Hôtel-Dieu de Lévis
101, rue du Mont-Marie,
Lévis (Québec) G6V 5C2
Canada
Phone: +1 418-835-7121, ext. 14642
jean-francois.cabana.cisssca@ssss.gouv.qc.ca

## Acknowledgments

The authors would like to thank everyone who contributed to this study, in particular Maryse Bélanger, radiation oncology therapist; Marie-Pier Cloutier, radiation oncology therapist; Marie-Pier Lagacé, radiation oncology therapist; Laurie Pilote, radiation oncologist; and every other colleagues at the CRIC who was involved in the study.

**References**

1 Bird, D., Henry, A. M., Sebag-Montefiore, D., Buckley, D. L., Al-Qaisieh, B., & Speight, R. (2019, November 1). A Systematic Review of the Clinical Implementation of Pelvic Magnetic Resonance Imaging–Only Planning for External Beam Radiation Therapy. International Journal of Radiation Oncology Biology Physics. Elsevier Inc. https://doi.org/10.1016/j.ijrobp.2019.06.2530
2 Siemens Healthcare GmbH. (2019). MR-only RT planning for the brain and pelvis with Synthetic CT.
3 Walker, A., Liney, G., Holloway, L., Dowling, J., Rivest-Henault, D., & Metcalfe, P. (2015). Continuous table acquisition MRI for radiotherapy treatment planning: Distortion assessment with a new extended 3D volumetric phantom. Medical Physics, 42(4), 1982–1991. https://doi.org/10.1118/1.4915920